Civil and Environmental Engineering
Vol. 21, Issue 2, 1232-1245, DOI: 10.2478/cee-2025-0091

STUDY OF ADHESION AT THE POLYMER-SILICATE COMPOSITE INTERFACE UNDER THE INFULENCE OF PHYSICO-MECHANICAL FACTORS

Nestor PLASTUN[1], Radoslav GANDEL[1*], Jan JERABEK[1], Oldrich SUCHARDA[1]

[1] Department of Building Materials and Diagnostics of Structures, Faculty of Civil Engineering, VSB - Technical University of Ostrava, Ludvika Podeste 1875/17, 708 00 Ostrava-Poruba, Czech Republic.
[*] corresponding author: radoslav.gandel@vsb.cz

Abstract

This paper investigates the potential of additive manufacturing for the production of polymer-based reinforcing elements designed to improve the structural properties and durability of silicate composites. The research addresses the interaction between polymer reinforcements and silicate composites, with a particular focus on the synergy at the material interface under physico-mechanical and environmental stresses. The aim is to increase both mechanical strength and resistance to degradation caused by water and chemical de-icing agents. Concrete composites reinforced with different 3D printed polymeric elements were experimentally tested for flexural and compressive strength as well as long-term durability. The results showed that optimized reinforcement geometry and material selection can lead to a significant improvement in composite properties. The high-performance concrete combined with appropriately designed polymer elements showed the greatest increase in compressive strength, while the conventional concrete benefited mainly in terms of flexural properties. In addition, some polymer reinforcements contributed to the maintenance of adhesive bonds even after prolonged exposure to aggressive environments. These findings confirm the viability of using additive manufacturing to create functional reinforcements tailored for cement-based materials, offering a new and adaptable approach to designing composites.

Keywords:

Polymer-silicate composite;
Polymer reinforcement element;
Adhesion;
Sustainability;
3D printing;
Additive technology.

1 Introduction

Concrete and reinforced concrete (RC) structures with conventional steel reinforcement are among the most widely used and extensively studied systems in engineering practice. Their robust performance has led to their widespread application in industrial and residential buildings, as well as in critical infrastructure. However, ongoing technological advances in the construction industry are increasingly focused on integrating traditional materials with modern manufacturing techniques to enhance structural performance, adaptability, and sustainability. One such emerging approach is the use of additive manufacturing - specifically 3D printing - for producing polymer reinforcement elements in cement-based composites [1–3]. While the behaviour of traditional concrete reinforcement systems, including dispersed and embedded steel or fiber reinforcements, has been thoroughly investigated [4–8], the introduction of 3D-printed polymer components offers new possibilities. These include the fabrication of reinforcement elements with virtually unlimited geometric configurations and the potential for small-scale, customized production using readily available desktop equipment. Nevertheless, a significant challenge remains: ensuring effective interaction between the polymer reinforcement and the concrete matrix. This interface critically influences the overall strength, stiffness, and long-term durability of the composite system. Factors such as mechanical loading, moisture ingress, chemical exposure, and temperature fluctuations can degrade this bond. Therefore, experimental research aimed at improving the physical and chemical compatibility at the polymer–concrete interface is essential to realizing the full potential of these novel hybrid materials.

As already mentioned, recyclability and degradability will play a key role in the future of the construction industry and, ultimately, in the sustainability of our planet. Conventional building materials, particularly Portland cement-based concretes [9], are expected to remain dominant in global construction for many years to come. However, their widespread use comes at a significant environmental cost, as CO_2 emissions from cement production [10–13] pose a serious threat to climate stability and the well-being of future generations. In response, the research community is intensifying efforts to find more sustainable alternatives [14–15]. At the same time, traditional concrete and reinforced concrete structures—despite their widespread use—face substantial limitations in long-term performance, especially under aggressive environmental exposure. These include corrosion of steel reinforcement [16], extensive cracking, shrinkage, and other degradation mechanisms that compromise durability and structural integrity. Such deterioration not only shortens service life and increases maintenance costs but can also result in major economic and safety-related consequences. In this context, it is necessary to approach the evaluation of degradation of existing structures as well as the design of new structures comprehensively and to use quantitative as well as qualitative methods as in [17] or strategic plans and frameworks such as in [18]. Therefore, in addition to addressing environmental impact, the development of alternative materials and systems must also aim to improve durability and resilience under demanding conditions.

One possible way to help reduce CO_2 emissions is to utilize everyday materials whose excessive accumulation poses a significant environmental burden. In addition to enriching traditional building materials with alternative raw materials such as waste glass [19], refractory concrete bricks [20] or textile fibres [21], it is also possible to use, for example polyethylene terephthalate (PET) from waste PET bottles, which has been also the subject of many studies, for example [22-24]. These works deal in detail with the replacement of the cementitious binder by an alternative binder made of resin from depolymerized waste PET material. Polyethylene terephthalate modified by glycol (PETG) is one of the most widely used materials in the field of polymer fused deposition modeling (FDM) 3D printing due to its strength (making it suitable for mechanically stressed components) and its relative ease of printability. Another polymer with potential applications is polylactic acid (PLA), a plant-based material that is valued for its biodegradability. However, its practical use is limited by several disadvantages compared to PETG, including lower thermal, mechanical and chemical resistance. As a result, PLA is primarily suitable for indoor use where exposure to aggressive environments is minimal. Nevertheless, PLA has found its role in many researches. For example, *Barkhad* [25] discusses the use of a PLA-based composite in the thermal insulation of buildings, achieving performance - both thermal and mechanical - comparable to that of conventional materials. *Nguyen-Van* [26], in turn, investigated the behaviour of a reinforced form of PLA lost formwork with cement mortar against dynamic loads. The results indicate a significant improvement in the load-bearing capacity of the concrete beams, suggesting potential applications in noise barriers, anti-vibration panels, and reinforced concrete structures exposed to environments with corrosive effects on steel reinforcement. *Chiadighikaobi* [27], on the other hand, used 3D printed PLA trusses as a reinforcing element of high-performance concrete. The best values were achieved by Warren's truss, which increased the maximum high-performance concrete (HPC) load by 14% while reducing the weight by approximately 3%. Other research [28, 29] exploited the relative brittleness of PLA in the use of capsules for bacteria in self-healing cementitious materials in optimizing the capsule rupture at the right moment. Among polymeric reinforcement materials previously investigated in literature, acrylonitrile butadiene styrene (ABS) has been recognized for its excellent toughness and heat resistance when combined with cementitious binders. Building upon these findings, the present study selected ABS as the third and final polymeric reinforcement material tested in ordinary Portland cement (OPC) and high-performance concrete (HPC) mixtures. *Palos* [30] in his work investigated the effect of ABS powder in cement mortar on the mechanical properties and adhesion to steel reinforcement. He concluded that ABS increases the compressive modulus of elasticity, but at the same time increases the porosity, thereby causing a decrease in the adhesion of cement mortar to steel reinforcement.

Therefore, the aim of this research is to assess the possibilities of interaction between polymer reinforcement elements and concrete matrix under different mechanical and environmental stress conditions. The experimental part includes testing of polymer-silicate composites based on high performance concrete and ordinary concrete with Portland cement. The polymer elements (PLA, PETG and ABS) were fabricated by 3D printing technology with different types of surface treatments, including smooth and ribbed plates or reinforcing square structures. The results of this study can contribute to the optimization of the design of polymer reinforcement elements and their incorporation into concrete structures. The knowledge gained may lead to the development of new composite materials with higher strength, better resistance to external influences and potentially reduce the environmental impact of construction technologies. At the same time, there is the possibility of wider application of additive manufacturing in the construction industry [31-33], which could contribute to more efficient and sustainable construction in the future.

2 Methodology

For the purpose of the experimental program of this paper, HPC and OPC mixtures were used, the composition of which is shown in Table 1. From a previous study [31], the results of granulometric tests of the fine-grained input materials and aggregates used are presented. In the case of 3D printed reinforcement elements made of PLA, PETG and ABS, the printing parameters were as follows (an example of printing is given in Figure 1):

- Filling: 20% (shape of grid)
- Layer height: 0.2 mm
- Print speed of perimeters: 80 mm/s
- Print speed of infill: 100 mm/s
- Operating temperature in the form “print bed temperature/nozzle temperature for the first layer/nozzle temperature for the following layers: PLA (60°C/215°C/210°C), PETG (85°C/230°C/240°C) and ABS (105°C/255°C/255°C)

Table 1: The composition of the used OPC and HPC mixtures.

Input materials	Amount [kg·m^{-3}]	
	OPC	HPC
CEM I 42.5 R, Hranice	450	-
CEM I 52.5 R, Hranice	-	650
Silica fume	-	70
Limestone finely ground, roughness of 8	-	80
Aggregate 0-4 mm, Tovacov	1230	890
Aggregate 4-8 mm, Litice	550	570
Polycarboxylate ether plasticizer	3	20
Polycarboxylate and polyphosphate plasticizer	-	10
Water	240	150

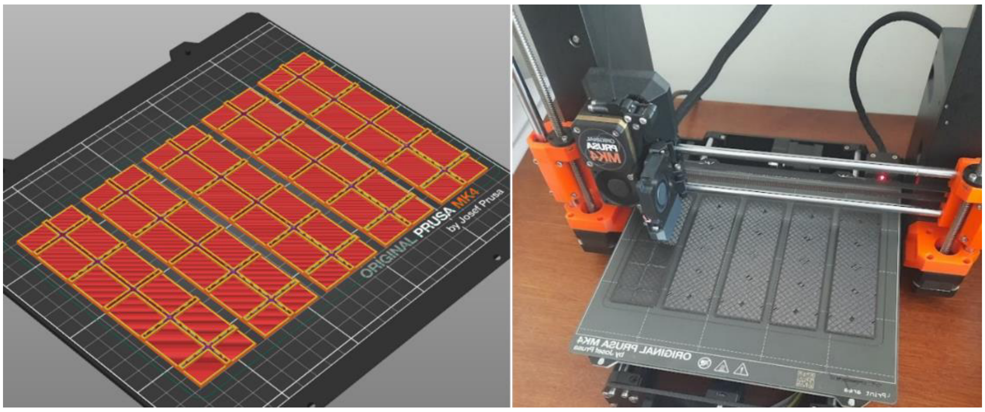

Fig. 1: Designed model and printing of reinforcement elements.

The polymer reinforcement elements consisted of two categories:

- Plates with dimension 2×40×140 mm; with smooth and ribbed surface (see Figure 2).
- Square reinforcement elements of 50×100×100 mm; without reinforcement and with two types of internal reinforcement 50×100×100 mm; (see Figure 3) located in the centre of the square reinforcement element, anchored in the walls, with wall thickness of 5 mm.

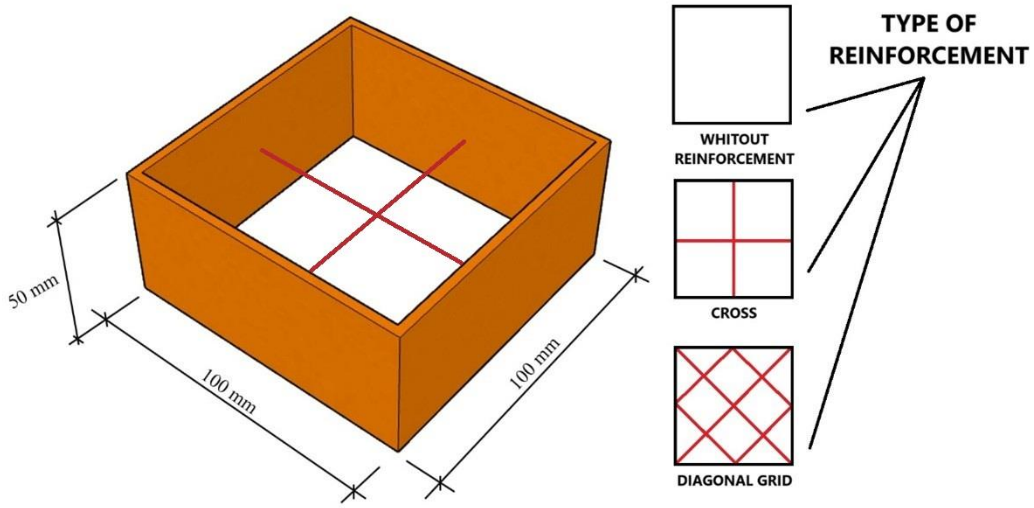

Fig. 2: Dimensions of the reinforcement element for 100x100x50 mm specimens and shapes of internal reinforcements.

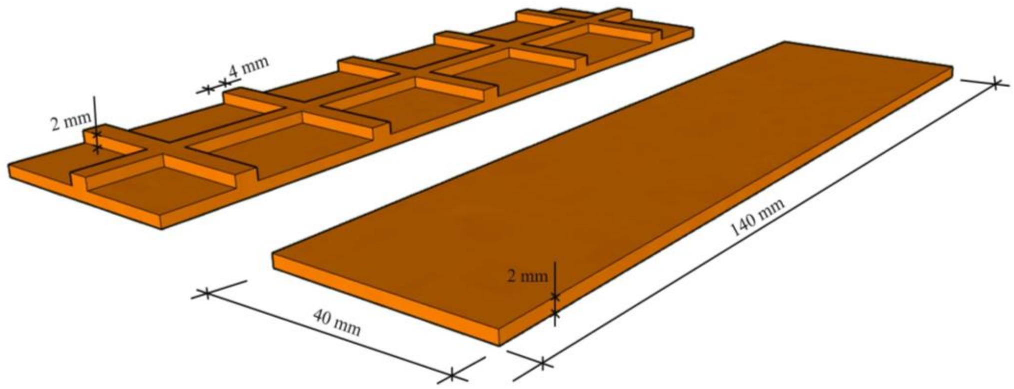

Fig. 3: Dimensions of the reinforcement element for prism specimens 40×40×160 mm.

Laboratory tests carried out as part of the experimental programme:

• *Compressive strength test* - Compressive strength test was carried out on 100 mm edge length cube specimens for the OPC and HPC mixtures and on 50×100×100 mm specimens for the polymer-silicate composite, with the lost formwork (see Figure 3) filled with both OPC and HPC mixtures with loading rate of (0.6 ± 0.2) MPa/s. Due to time constraints, not all possible combinations of reinforcement moulds and concrete mixtures were tested.

• *Flexural strength test* - 40×40×160 mm prism specimens of OPC, HPC and polymer-silicate composite mixtures (with two types of reinforcement elements) were tested with a three-point bending configuration, with a span between the bottom support rolls of 100 mm and a loading rate of (50 ± 10) N/s.

• *Resistance to water and chemical de-icing agents* – prisms with dimension of 40×40×160 mm prisms were tested for resistance to water and chemical de-icing agents according to the automatic cycling method: The specimens were immersed to a depth of (5 ± 1) mm in a 3 % NaCl solution, heated to a temperature of +20 °C and cooled to a temperature of -15 °C over a time period of 45-50 min, with a maximum temperatures maintained for 15 min, The prism specimens were placed in a test dish with the polymer reinforcement fully immersed in the solution (parallel to the water surface). No weight loss was detected during testing, and qualitative evaluation was performed every 25 cycles up to a total of 100 cycles. Both the degradation progression and the adhesion of the polymer-silicate composite components were assessed.

The specimens were subjected to testing 28 days after casting. For the 40×40×160 mm prisms, special care was taken during casting and compaction to prevent vertical displacement of the reinforcement element located at the bottom of the mould. To assess the bond behaviour without mechanical interlocks or adhesion promoters, smooth-surfaced reinforcement plates were used. The ribbed elements represent an initial attempt to achieve partial mechanical anchorage within the concrete. For square reinforcement components with integrated (lost) formwork, moulds had to be filled and compacted on a rigid, stable surface. It was also necessary to ensure sealing of the base of the mould to prevent leakage of the fresh concrete (a foil was used for this purpose after several trials). After 2 days, specimens were covered with foil to minimise evaporation during curing. During testing, in addition to reference mechanical performance values, failure modes and crack propagation were observed and recorded.

3 Results and discussion

3.1 Compressive strength of concrete mixes and polymer-silicate composites

The reference compressive strength of the OPC and HPC mixtures was determined using a series of four cube specimens with an edge length of 100 mm for each mixture. The average compressive strength values were 42.73 MPa for OPC and 118.24 MPa for HPC. Table 2 presents the results obtained from polymer-silicate composite specimens, which consisted of PLA square reinforcement moulds with dimensions of 50×100×100 mm and a wall thickness of 5 mm, filled with either OPC or HPC mixtures. The number of test specimens per mould type and mixture ranged from two to three.

Table 2: Compressive strength results of individual reinforcement moulds filled with OPC and HPC.

Mixture	Type of reinforcement	Peak compressive strength [MPa]	Residual Compressive strength [MPa]
OPC	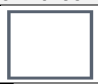	67.84	38.20
HPC		146.91	68.69
OPC		61.85	34.30
HPC		110.33	69.82
OPC	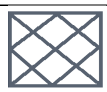	58.05	29.88
HPC		145.21	102.66

The peak compressive strength represents the average value at which the polymer moulds were disturbed without visible disturbance of the concrete parts. The residual compressive strength indicates the average value at which concrete failure and overall collapse of the polymer-silicate composites were evident.

• *Type of mould without internal reinforcement* - After reaching the peak compressive strength (67.84 MPa), the OPC specimens experienced failure of the polymer mould at the corner and failure of the edges of the concrete part. Subsequently, the concrete core continued to carry a reduced level of load, with a post-peak stress capacity of approximately 38.20 MPa, before complete failure of the composite structure. For HPC specimens, bulging of the mould walls was observed at a peak compressive stress of 146.91 MPa, with no apparent damage to the polymer formwork, suggesting improved interaction between the polymer and the high-performance concrete. After exceeding this stress level, the specimen failed at a stress of 68.69 MPa, corresponding to the ultimate load-bearing capacity of the composite assembly under compression.

• *Type of reinforcing mould with internal cross-shaped reinforcement* - In the case of OPC specimens, a slight decrease in both peak compressive stress and residual load-bearing capacity was observed, contradicting the initial assumption that internal wall anchorage would prevent mould failure. The maximum stress values were approximately 10% lower compared to specimens with moulds without internal reinforcement. A similar failure pattern was recorded, where the extruded mould initially cracked at one of its corners. For HPC specimens, the peak compressive stress was approximately 25% lower compared to the variant without internal reinforcement. However, the residual load-bearing capacity remained similar. In this configuration, the failure mode differed slightly: apart from mould cracking, partial delamination between the mould and the concrete core was also observed.

• *Type of reinforcing mould with internal grid-shaped reinforcement* - In this configuration, the OPC specimens exhibited the lowest peak compressive stress and residual load-bearing capacity, averaging 58.05 MPa and 29.88 MPa, respectively. The failure of the mould was characterized by partial collapse at the bottom due to inward deformation of the side walls. The HPC specimens showed similar behaviour and failure patterns as the OPC ones. While the peak compressive stress (145.21 MPa) was comparable to that of specimens with moulds lacking internal reinforcement, the residual load-bearing capacity was significantly higher—by approximately 30%—compared to the first two HPC configurations. A typical failure mode for this case is shown in Figure 4.

Fig. 4: The nature of the failure of the OPC specimen in the mould with a reinforcing grid.

When evaluating how the interaction between the polymer and concrete components affects compressive strength, the effect of specimen slenderness must be considered. Therefore, it is not possible to certainly quantify the compressive strength of the polymer-silicate composite and compare it with the results of the cubic compressive strengths of the reference specimens of the mixture used. Previous studies [33–36] have primarily focused on specimens with a height-to-diameter ratio (*h/d*) between 1.0 and 2.0, which is the standard range for evaluating compressive strength. However, for specimens with an *h/d* ratio below 1.0, the stress distribution and failure mechanisms differ significantly, and the available data are insufficient to accurately characterize their compressive behaviour. In such cases, not only the specimen size but also its shape becomes a critical factor. As highlighted by Qasim [37], low *h/d* ratio specimens typically fail by crushing, while higher ratios are associated with failure by cracking. This distinction is important for interpreting the results of compression tests involving non-standard specimen geometries. Using the relationship from Figure 5 [38] between the *h/d* ratio and the concrete strength, an increase in compressive strength of approximately 1.8 times can be expected, i.e. from 42.73 MPa to 76.92 MPa (OPC 100 mm reference cubes) and from 118.24 MPa to 212.83 MPa (HPC 100 mm reference cubes) for specimens with a loading area of 100×100 mm and a height of 50 mm. Most of the specimens in Table 2 would achieve these values if evaluated as a sum of peak and residual compressive strengths. In such a case, it could be argued that the proposed reinforcing PLA form of lost formwork has to some extent a positive effect on the compressive strength of the polymer-silicate composite.

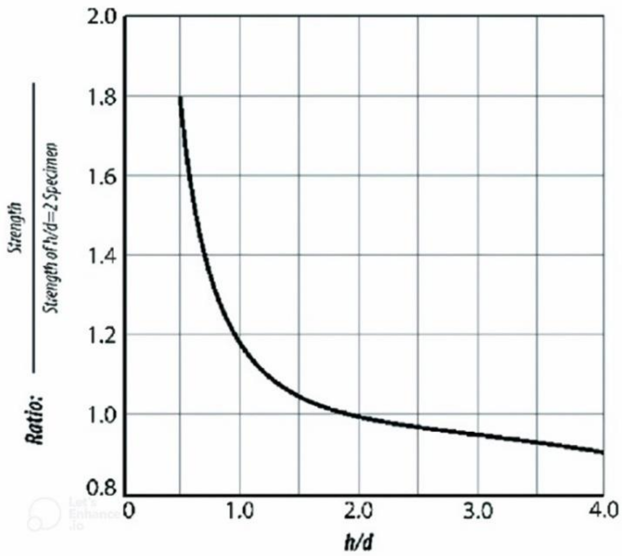

Fig. 5: The relationship between *h/d* ratio and strength characteristics of concrete [38].

3.2 Flexural strength

The 40×40×160 mm polymer-silicate prism specimens subjected to the three-point bending test were divided into several groups depending on polymer type, concrete mixture type, and reinforcement type. Again, the peak and residual flexural strengths were experimentally evaluated as well as the nature of failure. Each series of tests consisted of three specimens. For further comparison, the flexural strength of prismatic specimens made from the OPC and HPC reference mixtures is also presented. The testing was carried out on three specimens for each mixture using the same flexural test setup as for the reinforced composite specimens. Specimens of pure ordinary concrete based on Portland cement without reinforcement element achieved an average value of 6.76 MPa (indicated by the horizontal green line in the bar chart in Figure 6) and HPC ones 15.03 MPa (indicated by the horizontal blue line in the graph in Figure 6). The bar chart in Figure 6 provides a comprehensive overview of the results obtained.

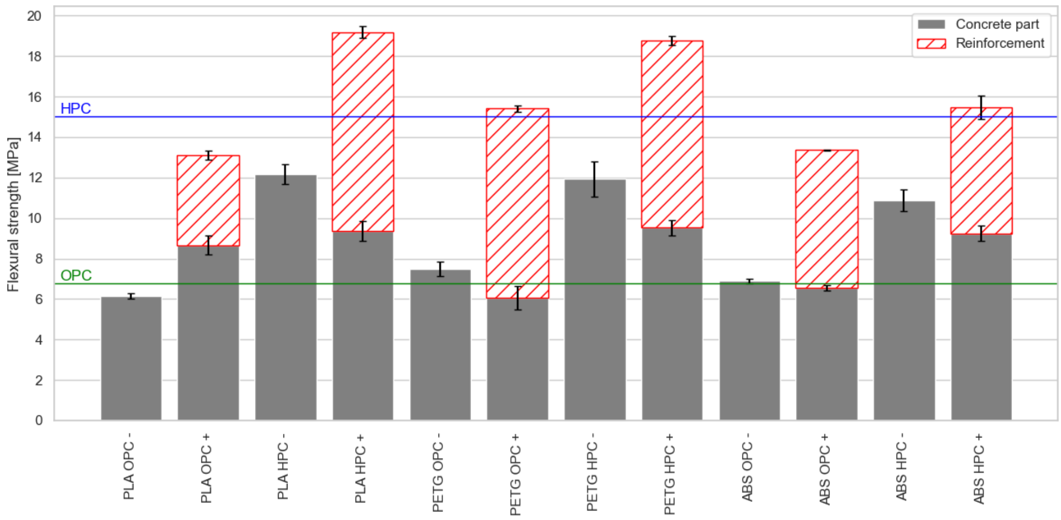

Fig. 6: Bar chart of flexural strengths of polymer-silicate prismatic specimens.

The much lower modulus of elasticity of the tested polymers, approximately 10% of the modulus of elasticity of concrete materials, means that the polymer reinforcement element is not able to effectively transfer tensile deformations as in the case of conventional reinforced concrete. The aim of this paper is not to replace the steel reinforcement with a polymeric variant, but to verify the interactions and adhesion of the different components of a polymer-silicate composite without an adhesion bridge. Therefore, the method of evaluating the flexural test results is not straightforward and may vary from author to author.

From the bar chart in Figure 6, the characteristic flexural behaviour of the polymer-silicate specimens can be distinguished based on the type of reinforcing element used. In general, both OPC and HPC specimens with a plain (non-anchored) reinforcing element exhibited complete composite failure upon reaching peak flexural load. This failure typically manifested either as a full cross-sectional fracture involving both the polymer and concrete components, or - more frequently - as failure of the concrete portion accompanied by loss of bond at the polymer-concrete interface, while the polymer structure itself remained structurally unaffected. This behaviour is illustrated in the bar chart presented in Figure 6, where the tested composite specimens are represented by segmented columns. Columns that contain only grey segments correspond to specimens with smooth reinforcement elements, while columns that include both grey and red-hatched segments represent specimens with ribbed reinforcement elements. The grey segments indicate the flexural strength associated with the initial (peak) failure of the concrete component. In the case of ribbed reinforcement, mechanical interlocking significantly enhanced the adhesion between the silicate matrix and the polymer reinforcement. For the specimens with ribbed elements (marked “+”), after the primary failure - manifested as a flexural crack in the concrete below the loading point - the integrity of the composite was preserved. The polymer reinforcement remained undamaged at this stage, and adhesion between the concrete and polymer components was maintained. These specimens were able to carry additional load until the polymer reinforcement eventually deformed and failed. This residual load-bearing capacity is represented by the red-hatched segments of the columns and corresponds to the residual flexural strength. Thus, in the case of ribbed reinforcement, the total flexural performance is interpreted as the sum of the peak and residual flexural strengths, reflecting the synergistic contribution of both components.

A slight improvement in flexural strength for the OPC mixture with a plain reinforcement element was observed for PETG material by approximately 10%. In the case of ABS, the results remained largely unchanged, whereas PLA exhibited lower performance compared to the OPC specimens without reinforcement elements. As for the HPC specimens with plain surface, in all three cases there was a decrease in flexural strength, which can be explained by the reduction of the cross-section of the HPC specimen and the replacement of this part by a less durable material. The flexural strengths were approximately 20-30 % lower than for the reference HPC specimens.

Specimens with the ribbed reinforcement element of the OPC mixture showed improvement in all cases. In the case of PLA reinforcement, a higher peak flexural strength compared to the reference OPC was observed by approximately 30% and the total flexural strength by approximately 90% at 13.11 MPa. The peak flexural strength of the OPC with PETG and ABS reinforcement was comparable to the reference OPC ones. However, the overall flexural strength of the PETG-reinforced OPC increased by almost 130 % (to 15,4 MPa) and that of the ABS-reinforced OPC by almost 100 % (to 13,36 MPa).

The HPC composites also demonstrated improved flexural performance compared to the reference prisms. Although the peak flexural strength values of the reinforced specimens did not exceed those of the unreinforced references, the combined flexural capacity - defined as the sum of peak and residual flexural strengths - surpassed the benchmark values. Specifically, HPC specimens reinforced with PLA elements achieved a total flexural capacity of 19.19 MPa, representing an increase of nearly 30% over the reference. For PETG-reinforced specimens, the improvement was approximately 25% (18.77 MPa), while ABS-reinforced specimens exhibited only a marginal increase of about 3% (15.47 MPa). Figure 7 presents photo documentation of the failure modes of OPC specimens with different polymer reinforcement elements. On the left, the image shows the OPC specimen reinforced with ABS, where delamination of the polymer occurred after the failure of the concrete portion. On the right, the OPC specimen with PETG reinforcement failed across the entire cross-section after reaching the maximum residual flexural strength. Despite this, the integrity of both the concrete and polymer components was preserved.

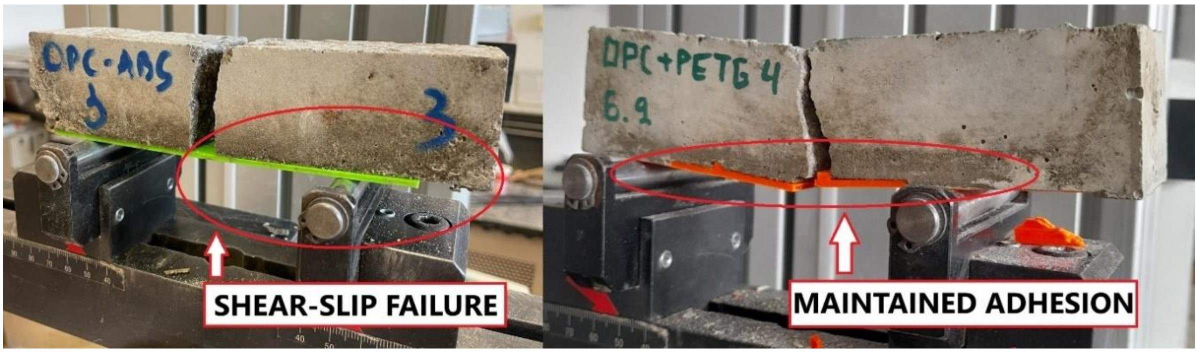

Fig. 7: Adhesion distortion while maintaining the integrity of the plain ABS polymer element in the OPC variant (left) and adhesion preservation of the PETG element and OPC part in the case of failure of the specimen by flexural testing.

There are not many studies that address the exact issue explored in this work; however, certain parallels can be drawn from related research. For example, *Patil* [39] investigated the effect of wrapping a 100×100×500 mm concrete beam with a 2 mm thick PLA film. Although an epoxy resin was used to enhance adhesion between the PLA and the beam, the results showed a slight improvement in the load-carrying capacity. In the present study, PLA-based composites exhibited improved flexural strength only in the case of specimens with ribbed reinforcement, highlighting the importance of mechanical interlocking. For PLA, effective adhesion - whether mechanical or chemical - is crucial for structural performance. Most existing studies on the adhesive behaviour of concrete composites with ABS, PETG, and PLA focus on the micro- or meso-scale and typically examine these polymers in powder or fiber form. Consequently, although some general trends can be identified, direct quantitative comparison of the present results with those in the literature remains limited due to differences in material form, reinforcement type, and testing conditions.

3.3 Resistance to water and chemical de-icing agents

The resistance of the specimens to water and chemical de-icing agents was not evaluated using the conventional method of measuring weight loss. Instead, a qualitative assessment of surface degradation was carried out after individual freeze-thaw cycles. This approach was chosen because the deteriorated material consisted of both concrete fragments and polymer debris from the three different reinforcement types, making mass loss measurements unreliable. The aim of this part of the experimental programme was to evaluate the impact of chemical de-icing agents on the integrity of the polymer-concrete adhesive bond, the durability of the polymer reinforcement itself, and its ability to limit the penetration of degradation agents into the concrete matrix. If favourable results are confirmed, the tested polymers could potentially be used as protective layers for concrete structures exposed to aggressive environments such as de-icing agents and moisture.

3.3.1 Evaluation after 25 freezing cycles

Already after 25 freeze–thaw cycles, the OPC-based specimens exhibited significant differences in performance depending on the type of reinforcement. Specimens with plain polymer reinforcement elements (PLA, PETG, ABS) showed complete detachment of the reinforcement from the concrete matrix, indicating insufficient interfacial bonding. In contrast, specimens with ribbed reinforcement demonstrated improved adhesion: ABS remained mechanically interlocked within the ribs despite concrete spalling at the edges, while PLA and PETG showed partial loss of polymer material and local debonding. HPC-based specimens, on the other hand, exhibited high durability across all reinforcement types, with no visible damage or interfacial failure. The bond between polymer and concrete remained intact, and no signs of degradation were observed. In summary, OPC specimens with plain reinforcement exhibited the lowest durability due to premature debonding and material degradation. Ribbed reinforcement improved adhesion, though some damage to the polymer was still observed. HPC specimens proved the most resistant, maintaining both structural and interfacial integrity after 25 cycles. OPC specimens with plain reinforcement elements were not subjected to further cycling due to advanced deterioration and complete bond failure. Figure 8 presents photographic documentation of the typical damage observed in the OPC specimens after 25 cycles.

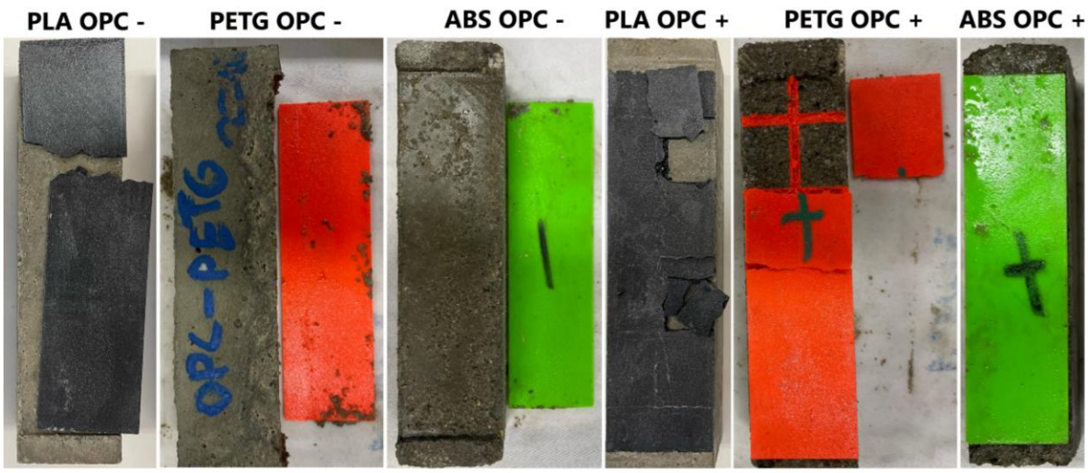

Fig. 8: Photo documentation of OPC specimens after exposure to 25 cycles of water and chemical thawing agents.

3.3.2 Evaluation after 50 freezing cycles

The OPC specimens with ribbed ABS reinforcement retained the adhesion between the polymer and concrete, but cracks and degradation of the concrete part of the composite appeared. The OPC specimens reinforced with ribbed PETG elements showed only minor degradation compared to the previous specimens. Local adhesion between the polymer and the concrete matrix was preserved, although micro-cracks were observed on the surface of the polymer reinforcement. The HPC specimens behaved comparatively more durable. The PETG ribbed element specimens remained without visible deterioration after 50 cycles, while the adhesion between concrete and polymer remained intact. The specimens with the ribbed PLA reinforcement element showed good adhesion, but minor cracking appeared. Plain ABS elements had poor adhesion and cracked, while specimens with ribbed ABS elements achieved higher durability without visible cracks. Overall, the best results were achieved by the ribbed PETG reinforcement elements, which remained intact. HPC specimens showed better adhesiveness compared to OPC, while plain PLA and ABS reinforcement elements were already more prone to cracking after 50 cycles. The PLA OPC composites were not subjected to additional cycles because the polymer-silicate composite had completely delaminated.

3.3.3 Evaluation after 75 freezing cycles

The OPC specimens with ribbed ABS reinforcement retained adhesion with the concrete part without cracking, but spalling occurred at the concrete surface. The HPC specimens with ribbed ABS elements remained intact, with no cracking. The smooth elements with PLA reinforcement retained adhesion with the concrete but a small crack appeared, while the ribbed PLA elements had cracks over the entire surface, although adhesion with the concrete was also maintained. The PETG elements, both plain and ribbed, did not show any damage, spalling or weakening of the adhesive bond. After 75 freeze-thaw cycles, the specimens with PETG reinforcement elements exhibited the most stable performance and remained structurally intact, with no visible signs of damage. The specimens with plain ABS retained high durability, but the OPC ones experienced concrete spalling and overall weakening of the adhesive bond. The PLA specimens with HPC were also adhesive, with the ribbed specimens exhibiting area cracks, but the bond to the concrete remained intact, as with the plain-surfaced variant.

3.3.4 Evaluation after 100 freezing cycles

The OPC specimens with ABS reinforcement exhibited good adhesion between the polymer and the concrete matrix, with no visible deterioration of the polymer itself; however, the concrete prisms showed signs of structural degradation. In contrast, HPC specimens with plain PLA reinforcement experienced complete delamination at the interface, indicating insufficient bonding. PETG-reinforced specimens demonstrated excellent adhesion performance across both plain and ribbed variants, without any observable material degradation or interfacial failure. Ribbed ABS reinforcements maintained a consistent bond with the concrete throughout testing. After 100 freeze–thaw cycles, the OPC specimens with ribbed ABS reinforcement still demonstrated adequate adhesion, although the concrete matrix had deteriorated to a degree that could compromise bond performance in prolonged exposure scenarios. Overall, higher resistance to cyclic freeze-thaw loading and exposure to chemical de-icing agents was observed for ABS and PETG polymers. In these cases, the combination of polymer stability and the inherent durability of HPC effectively prevented the ingress of degradation agents into the specimen. In contrast, PLA reinforcements showed low resistance to freeze-thaw conditions; the plain variants in particular cracked and delaminated during the early stages of testing. Among all tested materials, PETG demonstrated the highest long-term durability and consistent interfacial bonding with both OPC and HPC matrices. ABS also provided satisfactory results, but only in ribbed form. A typical failure pattern of HPC specimens after 100 freeze-thaw cycles is documented in Figure 9.

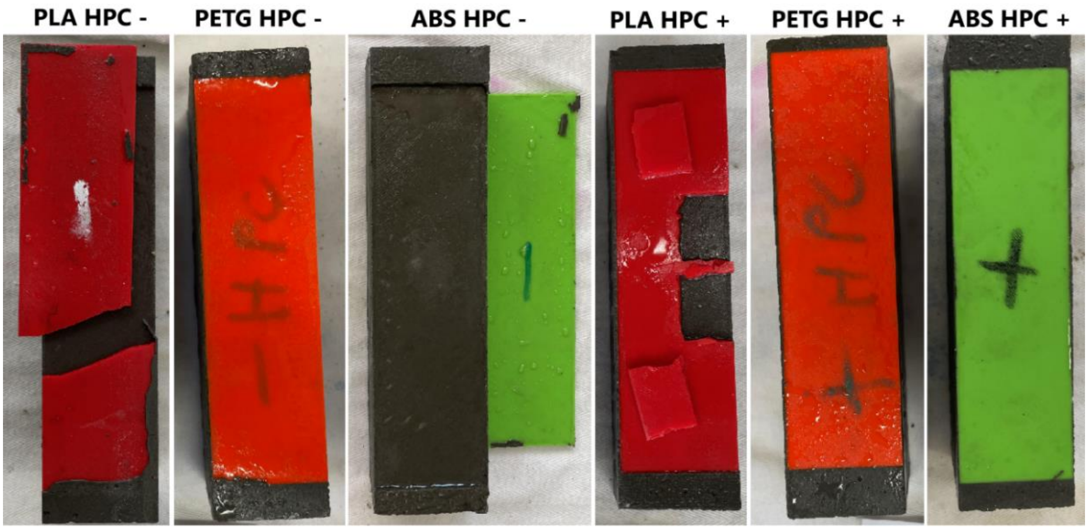

Fig. 9: Photo documentation of HPC specimens after exposure to 100 cycles of water and chemical thawing agents.

The following Table 3 provides a comprehensive view of the results of polymer-silicate composites after individual cycles of water and chemical de-icing agent resistance testing.

Table 3: Qualitative evaluation of the results of the resistance of polymer-silicate composites to water and chemical de-icing agents.

Polymer	Type of reinforcement	25 cycles		50 cycles		75 cycles		100 cycles	
		OPC	HPC	OPC	HPC	OPC	HPC	OPC	HPC
PLA	Plain	④	①	④	①	④	②	④	④
	Ribbed	③	①	④	①	④	②	④	③
PETG	Plain	④	①	④	①	④	①	④	①
	Ribbed	③	①	③	①	④	①	④	①
ABS	Plain	④	①	④	③	④	④	④	④
	Ribbed	①	①	①	①	①	①	①	①

Legend of symbols of Table 3:
① no visible defects, adhesion is maintained
② slight deterioration is visible - local cracks, adhesion is maintained
③ heavily damaged specimen, more cracks, adhesion is locally maintained
④ damaged specimen without maintaining adhesion at the polymer-silicate interface

From the results presented in Table 3, it can be concluded that the most effective polymer-silicate interactions were observed in specimens made with the HPC mixture. Among the tested reinforcement types, ribbed reinforcement elements proved to be the most effective, as their surface geometry enabled improved mechanical interlock within the concrete matrix. Among the polymeric materials tested, PETG demonstrated the highest resistance to moisture and chemical de-icing agents, with virtually no visible signs of degradation when combined with the HPC matrix. A comparable investigation into the durability of 3D-printed polymeric materials was carried out by *Moreno Nieto* [40], who examined the behaviour of PETG and PLA specimens immersed in saline solution. The study showed that PETG stabilized at a water absorption level of approximately 0.3% by weight after 9 weeks, while PLA reached a 2.5% increase in weight after just 8 weeks, along with significant evidence of surface degradation. These findings support the conclusions presented in the current study, confirming that PETG is the most suitable material for use in high-humidity or chemically aggressive environments, while PLA shows poor resistance and is therefore unsuitable for such conditions.

4 Conclusion

The study dealt with testing the adhesion of polymer-silicate composites under the influence of physico-mechanical factors with the following partial results:

• In the case of compressive strength, it was found that the reinforcing element with an internal reinforcing grid significantly increased the residual compressive strength of HPC compared to the specimens without internal reinforcement by about 30%, while the peak compressive strength was more or less maintained. For the OPC specimens, even the elements with internal reinforcement achieved a negative effect compared to the HPC ones with the reinforcing element without internal reinforcement. Thus, the strength of the silicate material is proportionally influenced by the interaction of the materials under compressive loading.

• Without additional anchoring elements, polymer-silicate composites with plain reinforcement did not appear to be suitable for obvious reasons, and the increase in flexural strength occurred only in the case of OPC with PETG. However, the ribbed reinforcement elements showed better results when, after reaching the peak flexural strength at which the concrete part failed, the integrity of the composite was maintained up to the maximum value of the residual compressive strength. In this case, PETG again proved to be the best material, showing almost 130% improvement in flexural strength when combined with OPC, but only about 25% in the case of HPC, outperformed by the PLA variant, which increased the flexural strength by about 30%.

• The water and chemical de-icing resistance test provided valuable information on the interactions of the tested polymers with OPC and HPC. The specimens with the ribbed reinforcement element again performed better. The PLA polymer was most susceptible to temperature changes, humid environment and saline solution. The ribbed ABS with HPC, although still retaining an adhesive bond after 100 cycles, exhibited small surface cracks. This phenomenon is probably due to the toughness of the polymer material. The PETG ribbed reinforcement held up best in almost all cases where it retained an intact structure. The problem was its bonding to the HPC, where the polymer was also largely damaged by significant degradation of the concrete part.

Overall, the composites with PETG exhibited the highest performance in both strength and durability tests. Thus, future research could involve a more detailed analysis of this material in conjunction with silicate building materials as well as its modified variant, such as PETG carbon. The data of the present experiment are presented in [41] and [42].

Acknowledgement

This research has been achieved with the financial support of the Ministry of Education, specifically by the Student Research Grant Competition of the Technical University of Ostrava under identification number SP2025/083. This paper was created also as part of the project No. CZ.02.01.01/00/22_008/0004631 Materials and technologies for sustainable development within the Jan Amos Komensky Operational Program financed by the European Union and from the state budget of the Czech Republic.

References

[1] SINGH, H., AMBEKAR, R. S., DAS, D., DANAM, V. A., KATIYAR, N. K., KANTI DAS, B., TIWARY, C. S., & BHATTACHARYA, J. (2024). Enhancing structural resilience by using 3D printed complex polymer reinforcement for high damage tolerant structures. *Construction and Building Materials*, 425, 136085. https://doi.org/10.1016/j.conbuildmat.2024.136085.

[2] HARRIS, M., RAZA, A., POTGIETER, J., IMDAD, A., RIMAŠAUSKIENĖ, R., & ARIF, K. M. (2023). 3D printed biodegradable polymer reinforced concrete with high structural stability. *Structures*, 51, 1609–1621. https://doi.org/10.1016/j.istruc.2023.03.156.

[3] SALAZAR, B., AGHDASI, P., WILLIAMS, I. D., OSTERTAG, C. P., & TAYLOR, H. K. (2020). Polymer lattice-reinforcement for enhancing ductility of concrete. *Materials & Design*, 196, 109184. https://doi.org/10.1016/j.matdes.2020.109184.

[4] SUCHARDA, O., MARCALIKOVA, Z., & GANDEL, R. (2022). Microstructure, Shrinkage, and Mechanical Properties of Concrete with Fibers and Experiments of Reinforced Concrete Beams without Shear Reinforcement. *Materials*, 15 (16), 5707. https://doi.org/10.3390/ma15165707.

[5] SUCHARDA, O., KONECNY, P., KUBOSEK, J., PONIKIEWSKI, T., & DONE, P. (2015). Finite Element Modelling and Identification of the Material Properties of Fibre Concrete. *Procedia Engineering*, 109, 234–239, https://doi.org/10.1016/j.proeng.2015.06.222.

[6] MATECKOVA, P., BILEK, V., & SUCHARDA, O. (2021). Comparative Study of High-Performance Concrete Characteristics and Loading Test of Pretensioned Experimental Beams. *Crystals*, 11, (4), 427). https://doi.org/10.3390/cryst11040427.

[7] GANDEL, R., JERABEK, J., & MARCALIKOVA, Z. (2023). Reinforced Concrete Beams Without Shear Reinforcement Using Fiber Reinforced Concrete and Alkali-Activated Material. *Civil and Environmental Engineering,* 19 (1), 348–356. https://doi.org/10.2478/cee-2023-0031.

[8] MARCALIKOVA, Z., JERABEK, J., GANDEL, R., GABOR, R., BILEK, V., & SUCHARDA, O. (2024). Mechanical Properties, Workability, and Experiments of Reinforced Composite Beams with Alternative Binder and Aggregate. *Buildings*, 14(7), 2142. https://doi.org/10.3390/buildings14072142.

[9] PEKNIKOVA, A., JERABEK, J., GANDEL, R., GABOR, R., BILEK, V., & SUCHARDA, O. (2025). Physical–Mechanical Behavior of High-Performance Concrete and Ordinary Concrete with Portland Cement Mixtures After Exposure to Selected Durability Tests Including High Thermal Stress. *Buildings*, 15 (7), 1029, https://doi.org/10.3390/buildings15071029.

[10] SCHNEIDER, M., ROMER, M., TSCHUDIN, M., & BOLIO, H. (2011). Sustainable cement production—present and future. *Cement and Concrete Research*, 41 (7), 642–650. https://doi.org/10.1016/j.cemconres.2011.03.019.

[11] HUNTZINGER, D. N., & EATMON, T. D. (2009). A life-cycle assessment of Portland cement manufacturing: comparing the traditional process with alternative technologies. *Journal of Cleaner Production*, 17 (7), 668–675. https://doi.org/10.1016/j.jclepro.2008.04.007.

[12] TURNER, L. K., & COLLINS, F. G. (2013). Carbon dioxide equivalent (CO2-e) emissions: A comparison between geopolymer and OPC cement concrete. *Construction and Building Materials*, 43, 125–130. https://doi.org/10.1016/j.conbuildmat.2013.01.023.

[13] JUENGER, M. C. G., WINNEFELD, F., PROVIS, J. L., & IDEKER, J. H. (2011). Advances in alternative cementitious binders. *Cement and Concrete Research*, 41 (12), 1232–1243. https://doi.org/10.1016/j.cemconres.2010.11.012.

[14] PROVIS, J. L. (2018). Alkali-activated materials. *Cement and Concrete Research*, 114, 40–48. https://doi.org/10.1016/j.cemconres.2017.02.009.

[15] SHI, C., JIMÉNEZ, A. F., & PALOMO, A. (2011). New cements for the 21st century: The pursuit of an alternative to Portland cement. *Cement and Concrete Research*, 41 (7), 750–763. https://doi.org/10.1016/j.cemconres.2011.03.016.

[16] KOPIIKA, N., BLIKHARSKYY, Y., SELEJDAK, J., KHMIL, R., & BLIKHARSKYY, Z. (2025). Reliability-based analysis and residual life forecasting for corrosion-affected RC structures. *Structures*, 76, 108965. https://doi.org/10.1016/j.istruc.2025.108965

[17] KRAMARCHUK, A., ILNYTSKYY, B., & KOPIIKA, N. (2023). Ensuring the load-bearing capacity of monolithic reinforced concrete slab damaged by cracks in the compressed zone. In Z. Blikharskyy (Ed.), Proceedings of EcoComfort 2022 (Lecture Notes in Civil Engineering, Vol. 290, pp. 185–192). Springer. https://doi.org/10.1007/978-3-031-14141-6_21

[18] KOPIIKA, N., ROBERY, P., NINIC, J., & MITOULIS, S.-A. (2025). Remaining life of ageing RC infrastructure for sustainable development—Deterioration under climate change. Case Studies in Construction Materials, 22, e04757. https://doi.org/10.1016/j.cscm.2025.e04757

[19] ISMAEEL, A. M., et al. (2024). Creating sustainable ultra-high-performance concrete (UHPC) utilizing recycled glass. *Civil and Environmental Engineering*, 20(2), 1152–1161. https://doi.org/10.2478/cee-2024-0084

[20] ABD, W. F., et al. (2025). Investigation the mechanical and physical characteristics of sustainable refractory concrete. *Civil and Environmental Engineering*, 0(0). https://doi.org/10.2478/cee-2025-0004

[21] HOANG, D. P., et al. (2025). Effect of short polypropylene fibre content on the mechanical properties of textile-reinforced engineered concrete composite. *Civil and Environmental Engineering*, 0(0). https://doi.org/10.2478/cee-2025-0039

[22] MAHDI, F., ABBAS, H., & KHAN, A. A. (2010). Strength characteristics of polymer mortar and concrete using different compositions of resins derived from post-consumer PET bottles. *Construction and Building Materials,* 24 (1), 25–36. https://doi.org/10.1016/j.conbuildmat.2009.08.006.

[23] MAHDI, F., ABBAS, H., & KHAN, A. A. (2013). Flexural, shear and bond strength of polymer concrete utilizing recycled resin obtained from post consumer PET bottles. *Construction and Building Materials*, 44, 798–811. https://doi.org/10.1016/j.conbuildmat.2013.03.081.

[24] KIM, J., JEONG, D., SON, C., LEE, Y., KIM, E., & MOON, I. (2007). Synthesis and applications of unsaturated polyester resins based on PET waste. *Korean Journal of Chemical Engineering,* 24 (6), 1076–1083. https://doi.org/10.1007/s11814-007-0124-5.

[25] BARKHAD, M. S., ABU-JDAYIL, B., IQBAL, M. Z., & MOURAD, A.-H. I. (2020). Thermal insulation using biodegradable poly(lactic acid)/date pit composites. *Construction and Building Materials*, 261, 120533). https://doi.org/10.1016/j.conbuildmat.2020.120533.

[26] NGUYEN-VAN, V., LIU, J., PENG, C., ZHANG, G., NGUYEN-XUAN, H., & TRAN, P. (2022). Dynamic responses of bioinspired plastic-reinforced cementitious beams. *Cement and Concrete Composites*, 133, 104682. https://doi.org/10.1016/j.cemconcomp.2022.104682.

[27] CHIADIGHIKAOBI, P. C., HASANZADEH, A., HEMATIBAHAR, M., KHARUN, M., MOUSAVI, M. S., STASHEVSKAYA, N. A., & ADEGOKE, M. A. (2024). Evaluation of the mechanical behavior of high-performance concrete (HPC) reinforced with 3D-Printed trusses. *Results in Engineering*, 22, 102058). https://doi.org/10.1016/j.rineng.2024.102058.

[28] RODRÍGUEZ, C. R., DE MENDONÇA FILHO, F. F., MERCURI, L., GAN, Y., ROSSI, E., ANGLANI, G., ANTONACI, P., SCHLANGEN, E., & ŠAVIJA, B. (2020). Chemo-physico-mechanical properties of the interface zone between bacterial PLA self-healing capsules and cement paste. *Cement and Concrete Research*, 138, 106228. https://doi.org/10.1016/j.cemconres.2020.106228.

[29] ŠAVIJA, B., FEITEIRA, J., ARAÚJO, M., CHATRABHUTI, S., RAQUEZ, J.-M., VAN TITTELBOOM, K., GRUYAERT, E., DE BELIE, N., & SCHLANGEN, E. (2016). Simulation-Aided Design of Tubular Polymeric Capsules for Self-Healing Concrete. *Materials*, 10 (1), 10). https://doi.org/10.3390/ma10010010.

[30] PALOS, A., D'SOUZA, N. A., SNIVELY, C. T., & REIDY, R. F., III. (2001). Modification of cement mortar with recycled ABS. *Cement and Concrete Research*, 31 (7), 1003–1007. https://doi.org/10.1016/s0008-8846(01)00531-2.

[31] SUCHARDA, O., GANDEL, R., CMIEL, P., JERABEK, J., & BILEK, V. (2024). Utilization of High-Performance Concrete Mixtures for Advanced Manufacturing Technologies. *Buildings* 14 (8), 2269. https://doi.org/10.3390/buildings14082269.

[32] LE, T. T., AUSTIN, S. A., LIM, S., BUSWELL, R. A., GIBB, A. G. F., & THORPE, T. (2012). Mix design and fresh properties for high-performance printing concrete. In *Materials and Structures,* 45 (8), 1221–1232. https://doi.org/10.1617/s11527-012-9828-z.

[33] LE, T. T., AUSTIN, S. A., LIM, S., BUSWELL, R. A., LAW, R., GIBB, A. G. F., & THORPE, T. (2012). Hardened properties of high-performance printing concrete. *Cement and Concrete Research,* 42 (3), 558–566. https://doi.org/10.1016/j.cemconres.2011.12.003.
[34] DEL VISO, J. R., CARMONA, J. R., & RUIZ, G. (2008). Shape and size effects on the compressive strength of high-strength concrete. *Cement and Concrete Research*, 38 (3), 386–395. https://doi.org/10.1016/j.cemconres.2007.09.020.
[35] SIM, J.-I., YANG, K.-H., KIM, H.-Y., & CHOI, B.-J. (2013). Size and shape effects on compressive strength of lightweight concrete. *Construction and Building Materials* 38, 854–864. https://doi.org/10.1016/j.conbuildmat.2012.09.073.
[36] VU, C.-C., WEISS, J., PLÉ, O., & AMITRANO, D. (2021). The potential impact of size effects on compressive strength for the estimation of the Young's modulus of concrete. *Materials and Structures*, 54 (5). https://doi.org/10.1617/s11527-021-01795-7.
[37] QASIM, O. A. (2018). A Review Paper on Specimens Size and Shape Effects on the Concrete Properties. In International Journal of Recent Advances in Science and Technology (Vol. 5, Issue 3). IJPBR. https://doi.org/10.30750/ijarst.533.
[38] TALAAT, A., EMAD, A., TAREK, A., MASBOUBA, M., ESSAM, A., & KOHAIL, M. (2021). Factors affecting the results of concrete compression testing: A review. *Ain Shams Engineering Journal* 12 (1), 205–221. https://doi.org/10.1016/j.asej.2020.07.015.
[39] PATIL, A. Y., BANAPURMATH, N. R., E. P., S., CHITAWADAGI, M. V., KHAN, T. M. Y., BADRUDDIN, I. A., & KAMANGAR, S. (2020). Multi-Scale Study on Mechanical Property and Strength of New Green Sand (Poly Lactic Acid) as Replacement of Fine Aggregate in Concrete Mix. *Symmetry* 12 (11), 1823. https://doi.org/10.3390/sym12111823.
[40] MORENO NIETO, D., ALONSO-GARCÍA, M., PARDO-VICENTE, M.-A., & RODRÍGUEZ-PARADA, L. (2021). Product Design by Additive Manufacturing for Water Environments: Study of Degradation and Absorption Behavior of PLA and PETG. *Polymers*, 13 (7), 1036. https://doi.org/10.3390/polym13071036.
[41] PLASTUN, N (2024). Adhesion of concrete composite with polymer elements from additive 3D printing technology, Diploma thesis. Ostrava: VSB – Technical University of Ostrava
[42] Experimental dataset. https://doi.org/10.5281/zenodo.14982019.